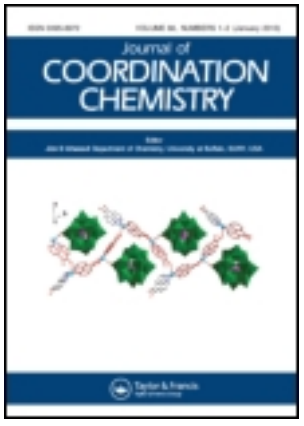

Journal of Coordination Chemistry
Publication details, including instructions for authors and subscription information:
http://www.tandfonline.com/loi/gcoo20

Solution and solid state studies with the bis-oxalato building block $[Cr(pyim)(C_2O_4)_2]^-$ [pyim = 2-(2′-pyridyl)imidazole]

Francisco R. Fortea-Pérez[a], Julia Vallejo[a], Mario Inclán[a], Mariadel Déniz[b], Jorge Pasán[b], Enrique García-España[a] & Miguel Julve[a]
[a] Instituto de Ciencia Molecular (ICMol)/Departamento de Química Inorgánica, Universitat de València, València, Spain
[b] Laboratorio de Rayos X y Materiales Moleculares, Departamento de Física Fundamental II, Facultad de Física, Universidad de La Laguna, Tenerife, Spain
Accepted author version posted online: 25 Aug 2013.Published online: 22 Oct 2013.

To cite this article: Francisco R. Fortea-Pérez, Julia Vallejo, Mario Inclán, Mariadel Déniz, Jorge Pasán, Enrique García-España & Miguel Julve (2013) Solution and solid state studies with the bis-oxalato building block $[Cr(pyim)(C_2O_4)_2]^-$ [pyim = 2-(2′-pyridyl)imidazole], Journal of Coordination Chemistry, 66:19, 3349-3364, DOI: 10.1080/00958972.2013.837460

To link to this article: http://dx.doi.org/10.1080/00958972.2013.837460

Journal of Coordination Chemistry, 2013
Vol. 66, No. 19, 3349–3364, http://dx.doi.org/10.1080/00958972.2013.837460

Solution and solid state studies with the bis-oxalato building block $[Cr(pyim)(C_2O_4)_2]^-$ [pyim = 2-(2′-pyridyl)imidazole]

FRANCISCO R. FORTEA-PÉREZ†, JULIA VALLEJO†, MARIO INCLÁN†, MARIADEL DÉNIZ‡, JORGE PASÁN‡, ENRIQUE GARCÍA-ESPAÑA† and MIGUEL JULVE*†

†Instituto de Ciencia Molecular (ICMol)/Departamento de Química Inorgánica, Universitat de València, València, Spain
‡Laboratorio de Rayos X y Materiales Moleculares, Departamento de Física Fundamental II, Facultad de Física, Universidad de La Laguna, Tenerife, Spain

(*Received 5 July 2013; accepted 5 August 2013*)

The preparation, X-ray structure, and variable temperature magnetic study of the new compound $\{Ba(H_2O)_{3/2}[Cr(pyim)(C_2O_4)_2]_2\}_n \cdot 9/2nH_2O$ (**1**) [pyim = 2-(2′-pyridyl)imidazole and $C_2O_4^{2-}$ = dianion of oxalic acid], together with the potentiometric and spectrophotometric studies of the protonation/deprotonation equilibria of the pyim ligand and the ternary complex $[Cr(pyim)(C_2O_4)_2]^-$, are reported herein. The crystal structure of **1** consists of neutral chains, with diamond-shaped units sharing barium(II), with the two other corners occupied by chromium(III). The two metal centers are connected through bis(bidentate) oxalate. Very weak antiferromagnetic interactions between the chromium(III) ions occur in **1**. The values of the protonation constants of the imidazole and pyridyl fragments of pyim as well as the acidity constant of the coordinated pyim in $[Cr(pyim)(C_2O_4)_2]^-$ are determined for the first time by potentiometry and UV–Vis spectroscopy in aqueous solution (25 °C and 0.15 M $NaNO_3$ as ionic strength).

Keywords: Chromium(III); Barium(II); Crystal structure; 2-(2′-Pyridyl)imidazole; Magnetic properties; Acidity equilibria

1. Introduction

One of the best preparative routes to heterobimetallic species is the so-called metal-as-ligand strategy, that is, the use of a stable complex (building block) that can act as a ligand towards fully solvated metal ions or preformed species whose coordination sphere is unsaturated. Cyanide oxalate- and oxamidate/oxamate-containing metal complexes are among the most representative examples of the success of this strategy [1–4]. Within this framework, the heteroleptic complex $[Cr(AA)(C_2O_4)_2]^-$ [AA = 2,2′-bipyridine (bipy), 1,10-phenanthroline (phen), 2,2′-dipyridylamine (dpa), 4,4′-dimethylbipyridine (dmbpy), 2,2′-bipyrimidine (bpym) and histamine (hm)] has been proved to be a very useful candidate [5]. Several features account for its ability to generate heterometallic compounds: (i) its stability in solution due to the reluctance of the Cr(III) species to undergo ligand exchange; (ii) its negative charge which is an important point regarding the cation assembling; (iii) the

*Corresponding author. Email: miguel.julve@uv.es

presence of two potential bis(chelating) oxalate groups; (iv) the added functionalities represented by the chelating AA molecule (supramolecular interactions, potential bridging ligand, etc.); (v) and the variety of univalent organic and inorganic cations that can be used to isolate it, the solubility of the resulting compound in different solvents being strongly dependent on the nature of the precipitating cation.

Let us briefly comment about the structural results obtained through the use of the $[Cr(AA)(C_2O_4)_2]^-$ unit as a building block for metal assembling in the cases of alkaline- [68] and alkaline-earth metal ions [9–11]. The reaction of $[Cr(bpym)(C_2O_4)_2]^-$ with sodium(I) and potassium(I) afforded 2-D neutral networks $[NaCr(bpym)(C_2O_4)_2]_n \cdot 5nH_2O$ [6a] and $[K(H_2O)Cr(bpym)(C_2O_4)_2]_n$ [6b]. The $[Cr(bpym)(C_2O_4)_2]^-$ unit in the former compound adopts a tris-bidentate coordination mode yielding a honeycomb-layered structure, where the sodium(I) cations are six-coordinate. However, the bpym and one of the two oxalate groups in the second compound also exhibit the bis-bidentate coordination mode but the remaining oxalate adopts the bis-bidentate/monodentate(outer) bridging mode, and the potassium(I) is nine-coordinate. This structural difference between the sodium and potassium derivatives is also observed when bpym in the chromium(III) unit is replaced by the bipy or phen molecules [7]. In these cases, the 2-D compounds $[Na(H_2O)Cr(phen)(C_2O_4)_2]_n \cdot 0.5nH_2O$ [7a], $[Na(H_2O)Cr(bipy)(C_2O_4)_2]_n \cdot 2nH_2O$ [7b], and $[K(dmf)Cr(phen)(C_2O_4)_2]_n \cdot 0.5nH_2O$ [7a] were obtained where the univalent cations are six-coordinate and the oxalate groups act as bridging ligands [bis-bidentate and bis-bidentate/monodentate(outer) in the sodium derivatives and bis-bidentate/monodentate(outer) and bidentate/bis-monodentate(outer) in the potassium salt]. Finally, with alkaline-earth cations, the $[Cr(AA)(C_2O_4)_2]^-$ unit with AA = bipy [8], phen [8b], dpa [9], or dmbpy [10] adopts the coordination modes shown in scheme 1, the structures of the heterobimetallic compounds being 1-D, 2-D, or 3-D.

As a continuation of the previous work on the use of the 2-(2′-pyridyl)imidazole (pyim, see scheme 2) as the AA ligand [11], we focus here on the coordinating behavior of the heteroleptic $[Cr(pyim)(C_2O_4)_2]^-$ *versus* barium(II) as well as on the study of the possibility to deprotonate the imidazole fragment of the coordinated pyim, a feature that would increase the negative charge and the complexing capability of this mixed-ligand species.

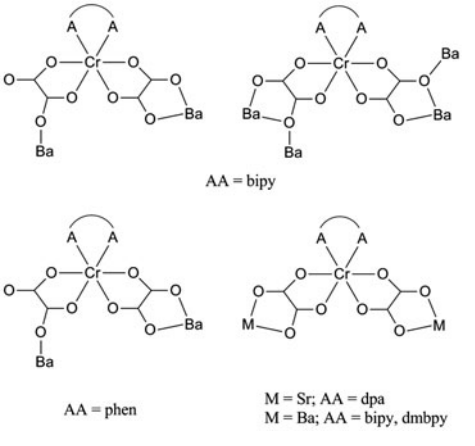

Scheme 1.

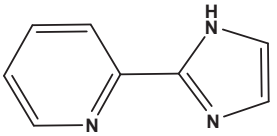

HL

Scheme 2.

2. Experimental

2.1. *Materials*

Chromium(III) chloride hexahydrate, sodium oxalate, tetraphenylphosphonium chloride, and barium(II) chloride dihydrate were purchased from commercial sources and used as received. $PPh_4[Cr(pyim)(C_2O_4)]\cdot H_2O$ and pyim were prepared by following previously reported procedures [11].

2.2. *Physical techniques*

2.2.1. Solid samples. Elemental analysis (C, H, N) of **1** was performed by the Servicio Central de Investigación Científica of the University Jaume I at Castellón. The value of the Cr:Ba molar ratio in **1** (2:1) was determined by electron microscopy at the Servicio Central de Soporte a la Investigación Experimental (SCSIE) of the University of Valencia. The IR spectrum (4000–400 cm^{-1}) of **1** was performed with a Bruker IF S55 spectrophotometer on a sample prepared as a KBr pellet. Thermal analysis of **1** was carried out on a Mettler Toledo TGA/SDT A851 apparatus using 3 mg of sample placed on a platinum pan and run under a dinitrogen atmosphere from 25–400 °C, the rate being 10 °C min^{-1}. The magnetic susceptibility of a polycrystalline sample of **1** was measured with a Quantum Design SQUID susceptometer from 1.9–295 K using applied magnetic fields of 0.5 T ($T > 30$ K) and 250 G ($T \leq 30$ K). Diamagnetic corrections of the constituent atoms were estimated from Pascal's constants [12] and found to be -211×10^{-6} $cm^3\,mol^{-1}$ [per one chromium (III)]. Corrections for the sample holder were also applied.

2.2.2. Solution samples. The potentiometric titrations were carried out at 298.1 ± 0.1 K using 0.15 M $NaNO_3$ as the supporting electrolyte. The experimental procedure (burette, potentiometer, cell, stirrer, microcomputer, etc.) has been fully described elsewhere [13]. The acquisition of the EMF data was carried out with the computer program PASAT [14]. The reference electrode was a Ag/AgCl electrode in saturated KCl solution. The glass electrode was calibrated as a hydrogen ion concentration probe by titration of previously standardized amounts of HCl with CO_2-free NaOH solutions and the determination of the equivalent point by Gran's method [15], which gives the standard potential E^0 and the ionic product of water [$pK_w = 13.73(1)$]. The computer program HYPERQUAD was used to calculate the protonation and stability constants from the titration curves [16]. The pH ranges investigated were 2.5–10.5 and 6.0–10.5 for HL and the Cr(III) complex, respectively. The concentration of the ligand and the complex ranged from 7.0×10^{-4} to a maximum value of 2.0×10^{-3} M. The different titration curves for each system (at least two) were treated either as a single set or as separated curves without significant variations in the values of the stability constants. The sets of data were merged together and treated simultaneously to give the final stability constants.

Absorption spectra were recorded with an UV/Vis spectrophotometer. HCl and NaOH were used to adjust the pH values, which were recorded with a calibrated pH meter. All solutions were prepared using miliQ water as solvent. The computer program HypSpec [16] was used to calculate the stability constants from the titration spectral data.

2.3. *Synthesis of $\{Ba(H_2O)_{3/2}[Cr(pyim)(C_2O_4)_2]_2\}_n \cdot 9/2nH_2O$ (1)*

Chromium(III) chloride hexahydrate (1.33 g, 5 mmol) and pyim (0.725 g, 5 mmol) were dissolved in 50 mL of water and refluxed for 4 h under continuous stirring. Solid sodium oxalate (1.34 g, 10 mmol) was added and the reflux was continued for 2 h. The resulting deep purple solution was filtered to remove any small amount of precipitate and allowed to cool at room temperature. Barium(II) chloride (0.52 g, 2.5 mM) dissolved in a minimum amount of water was poured into this solution under stirring and then allowed to evaporate at room temperature. Deep red parallelepipeds of **1** were grown after three days. They were collected by filtration, washed with a small amount of cold water, and air-dried. The yield is *ca.* 65%. Anal. Calcd for $C_{24}H_{26}BaCr_2N_6O_{22}$ (**1**): C, 29.05; H, 2.62; N, 8.47. Found: C, 28.91; H, 2.55; N, 8.35%.

2.4. *X-ray crystallography*

Diffraction data on single crystals of **1** were collected with an Agilent Supernova μ-focus diffractometer at 293(2) K using Cu radiation (λ = 1.5418 Å). Crystal parameters and refinement results for **1** are listed in table 1. The data collection was carried out with ω

Table 1. Crystal data and structure refinement parameters for $\{Ba(H_2O)_{3/2}[Cr(pyim)(C_2O_4)_2]_2\}_n \cdot 9/2nH_2O$ (**1**).

Empirical formula	$C_{24}H_{26}N_6O_{22}BaCr_2$
Formula weight	991.75
Crystal size (mm^3)	0.15 × 0.08 × 0.07
Crystal system	Triclinic
Space group	$P(-1)$
Unit cell dimensions (Å, deg)	
a	9.6742(7)
b	11.1929(7)
c	17.5740(12)
α	89.771(5)
β	80.285(6)
γ	75.248(6)
Volume ($Å^3$, Z)	1813.9(2), 2
Calculated density (g cm^{-3})	1.987
Absorption coefficient (mm^{-1})	14.084
$F(000)$	960
θ range (deg)	4.08–70.57
Index ranges	$-11 \le h \le 10$
	$-13 \le k \le 13$
	$-18 \le l \le 21$
Independent reflections (R_{int})	6717 (0.0421)
Observed reflections [$I \ge 2\sigma(I)$]	4682
Goodness-of-fit on F^2	1.045
Final R indices [$I \ge 2\sigma(I)$]	R_1 = 0.0787, wR_2 = 0.2030
R indices (all data)	R_1 = 0.1044, wR_2 = 0.2285
Largest diff. peak/hole (e $Å^{-3}$)	1.728/−2.298

scans in the θ range 4.08–70.57°. Data were indexed, scaled, and integrated using the Agilent CrysalisPro software [17]. The structure of **1** was solved by direct methods and refined with full-matrix least-squares technique on F^2 including all reflections and using the SHELXS-97 and SHELXL-97 programs [18] included in the WINGX software package [19]. All non-hydrogen atoms were refined anisotropically. The hydrogen atoms were geometrically positioned and refined using a riding model, except those of the water which

Table 2. Selected interatomic bond lengths (Å) and angles (°) for **1**.*

Cr(1)–O(1)	1.967(6)	Cr(2)–N(5)	1.991(12)
Cr(1)–O(3)	1.977(6)	Ba(1)–O(2)	2.792(7)
Cr(1)–O(5)	1.962(6)	Ba(1)–O(4)	2.874(7)
Cr(1)–O(7)	1.952(7)	Ba(1)–O(6b)	2.806(8)
Cr(1)–N(1)	2.069(8)	Ba(1)–O(8b)	2.817(8)
Cr(1)–N(2)	2.021(7)	Ba(1)–O(10)	2.858(8)
Cr(2)–O(9)	1.960(8)	Ba(1)–O(12)	2.759(9)
Cr(2)–O(11)	1.953(8)	Ba(1)–O(14a)	2.804(9)
Cr(2)–O(13)	1.967(8)	Ba(1)–O(16a)	2.741(5)
Cr(2)–O(15)	1.967(14)	Ba(1)–O(1w)	2.838(11)
Cr(2)–N(4)	2.050(7)	Ba(1)–O(7w)	2.996(16)
O(1)–Cr(1)–O(3)	82.9(2)	O(2)–Ba(1)–O(7w)	115.4(5)
O(1)–Cr(1)–O(5)	90.7(2)	O(4)–Ba(1)–O(6b)	69.8(2)
O(1)–Cr(1)–O(7)	92.3(3)	O(4)–Ba(1)–O(8b)	83.0(2)
O(1)–Cr(1)–N(1)	93.7(3)	O(4)–Ba(1)–O(10)	142.1(3)
O(1)–Cr(1)–N(2)	172.9(3)	O(4)–Ba(1)–O(12)	135.3(3)
O(3)–Cr(1)–O(5)	171.4(3)	O(4)–Ba(1)–O(14a)	126.0(2)
O(3)–Cr(1)–O(7)	91.7(3)	O(4)–Ba(1)–O(16a)	75.4(3)
O(3)–Cr(1)–N(1)	90.5(3)	O(4)–Ba(1)–O(1w)	117.0(3)
O(3)–Cr(1)–N(2)	94.0(3)	O(4)–Ba(1)–O(7w)	75.2(5)
O(7)–Cr(1)–O(5)	82.7(3)	O(6b)–Ba(1)–O(8b)	59.1(2)
O(7)–Cr(1)–N(1)	173.8(3)	O(6b)–Ba(1)–O(10)	74.5(2)
O(7)–Cr(1)–N(2)	94.2(3)	O(6b)–Ba(1)–O(12)	123.4(3)
O(5)–Cr(1)–N(1)	95.7(3)	O(6b)–Ba(1)–O(14a)	145.1(2)
O(5)–Cr(1)–N(2)	93.0(3)	O(6b)–Ba(1)–O(16a)	145.0(3)
N(1)–Cr(1)–N(2)	79.9(3)	O(6b)–Ba(1)–O(1w)	75.6(4)
O(9)–Cr(2)–O(11)	83.5(4)	O(6b)–Ba(1)–O(7w)	117.2(4)
O(9)–Cr(2)–O(13)	90.6(3)	O(8b)–Ba(1)–O(10)	67.7(3)
O(9)–Cr(2)–O(15)	92.4(5)	O(8b)–Ba(1)–O(12)	73.5(3)
O(9)–Cr(2)–N(4)	172.5(6)	O(8b)–Ba(1)–O(14a)	143.6(3)
O(9)–Cr(2)–N(5)	93.0(5)	O(8b)–Ba(1)–O(16a)	120.1(4)
O(11)–Cr(2)–O(13)	172.0(5)	O(8b)–Ba(1)–O(1w)	120.3(3)
O(11)–Cr(2)–O(15)	91.6(6)	O(8b)–Ba(1)–O(7w)	66.4(5)
O(11)–Cr(2)–N(4)	97.9(4)	O(10)–Ba(1)–O(12)	59.3(2)
O(11)–Cr(2)–N(5)	91.6(6)	O(10)–Ba(1)–O(14a)	91.0(3)
O(13)–Cr(2)–O(15)	83.0(4)	O(10)–Ba(1)–O(16a)	140.0(3)
O(13)–Cr(2)–N(4)	88.7(3)	O(10)–Ba(1)–O(1w)	64.1(3)
O(13)–Cr(2)–N(5)	94.0(5)	O(10)–Ba(1)–O(7w)	111.6(5)
O(15)–Cr(2)–N(4)	94.9(5)	O(12)–Ba(1)–O(14a)	70.2(3)
O(15)–Cr(2)–N(5)	173.9(4)	O(12)–Ba(1)–O(16a)	84.3(3)
N(4)–Cr(2)–N(5)	79.6(5)	O(12)–Ba(1)–O(1w)	107.6(4)
O(2)–Ba(1)–O(4)	58.49(19)	O(12)–Ba(1)–O(7w)	60.8(5)
O(2)–Ba(1)–O(6b)	87.7(2)	O(14a)–Ba(1)–O(16a)	59.2(4)
O(2)–Ba(1)–O(8b)	136.9(12)	O(14a)–Ba(1)–O(1w)	69.6(4)
O(2)–Ba(1)–O(10)	132.9(2)	O(14a)–Ba(1)–O(7w)	97.6(4)
O(2)–Ba(1)–O(12)	147.9(3)	O(16a)–Ba(1)–O(1w)	119.3(4)
O(2)–Ba(1)–O(14a)	79.3(2)	O(16a)–Ba(1)–O(7w)	54.3(5)
O(2)–Ba(1)–O(16a)	71.2(3)	O(1w)–Ba(1)–O(7w)	165.8(5)
O(2)–Ba(1)–O(1w)	69.4(3)		

*Symmetry transformations used to generate equivalent atoms: (a) $x + 1, y, z$; (b) $x-1, y, z$.

were neither found nor set. A water molecule [O(5w)] was disordered into two positions, their site occupancy factors refined with values 0.71 [O(5w)] and 0.29 [O(5wb)]. The water molecules O(6w) and O(7w) were refined with occupancy factors of 0.5. Some distance restraints were applied to pyim, which is somewhat disordered with slightly large ADPs. The final geometrical calculations and the graphical manipulations were carried out with PARST95 [20] and DIAMOND [21] programs. Selected bond lengths and angles for **1** are given in table 2.

3. Results and discussion

3.1. *FT-IR Spectroscopy and TG analysis of 1*

The high frequency region of the IR spectrum of **1** exhibits a broad and strong absorption at 3600–3250 cm^{-1} [ν(OH) + ν(NH)] due to the occurrence of uncoordinated and coordinated water and the N–H stretch of pyim linked by hydrogen bonds [22]. Several weak intensity peaks from 3150–2920 cm^{-1} [ν(C–H) stretch] and weak absorptions at 755 and 705 (out-of-phase C–H bending) are the signature of the presence of pyim. Strong peaks at 1712, 1680, and 1658 cm^{-1} [ν_{as}(CO)], together with the medium intensity absorptions at 795 [δ(OCO)], 898 [ν_{as}(Ba–O_{ox})], and 530 cm^{-1} [ν_{as}(Cr–O_{ox})], support the presence of coordinated oxalate [23, 24].

The thermogravimetric analysis of **1** is shown in figure S1. The complex undergoes weight loss in two steps. The initial loss occurs between room temperature and 130 °C and corresponds to six water molecules (obs. wt. loss: 11.0; Calcd wt. loss: 10.90%) yielding the anhydrous species. The dehydrated complex does not undergo any appreciable mass loss between 130 and 330 °C. On heating above 330 °C, it exhibits a rapid decomposition which was not further investigated.

3.2. *Crystal structure of 1*

Compound **1** crystallizes in the triclinic $P(-1)$ space group. Its structure consists of crystallographically independent heterotrinuclear units $\{Ba(H_2O)_{3/2}[Cr(pyim)(C_2O_4)_2]_2\}$ (figure 1) that grow along the crystallographic *a* axis through oxalate bridges to afford homochiral double zigzag chains (figure 2). Each chain is formed of diamond-shaped units sharing barium(II) ion, while the other two corners are filled by chromium(III). The adjacent double chains are related by an inversion center leading to an achiral structure. The same topology of the metal centers in **1** was previously observed for structures of the heterobimetallic compounds $\{Mn[Cr(bipy)(C_2O_4)_2]_2\}_n$ [8a], $\{Sr[Cr(dpa)(C_2O_4)_2]_2\}_n \cdot 8nH_2O$ [9], $\{Ba(H_2O)_2[Cr(bipy)(C_2O_4)_2]_2\}_n \cdot 4nH_2O$ [8b], and $\{Ba(H_2O)_2[Cr(dmbipy)(C_2O_4)_2]_2\}_n \cdot 17/2nH_2O$ [10]. The neutral double chains of opposite chirality in **1** are interconnected by π–π interactions between pyim molecules leading to supramolecular layers extending in the (01–2) plane (figure 2). Two types of these stacking interactions (imidazolyl···imidazolyl and pyridyl···pyridyl) are regularly alternated along the *a* axis [the centroid–centroid distance between the imidazolyl rings and the offset angle are 4.4853(3) Å and 25.0(3)°, respectively, whereas the corresponding ones for the pyridyl rings are 4.2232(3) Å and 25.6(3)°]. The crystallization water molecules occupy the interlayer space and connect the supramolecular layers through an extensive network of hydrogen bonds with the coordinated

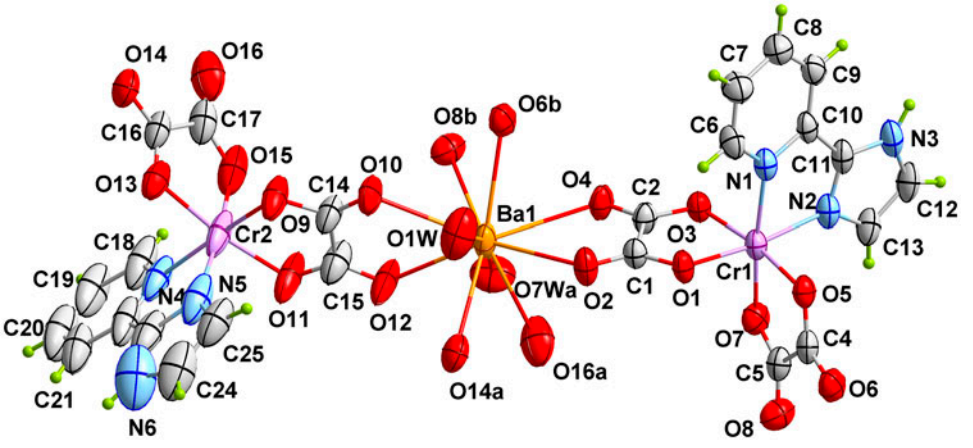

Figure 1. Perspective view of the crystallographically independent heterotrinuclear $Ba^{II}Cr^{III}_2$ unit of **1** with the labeling scheme.

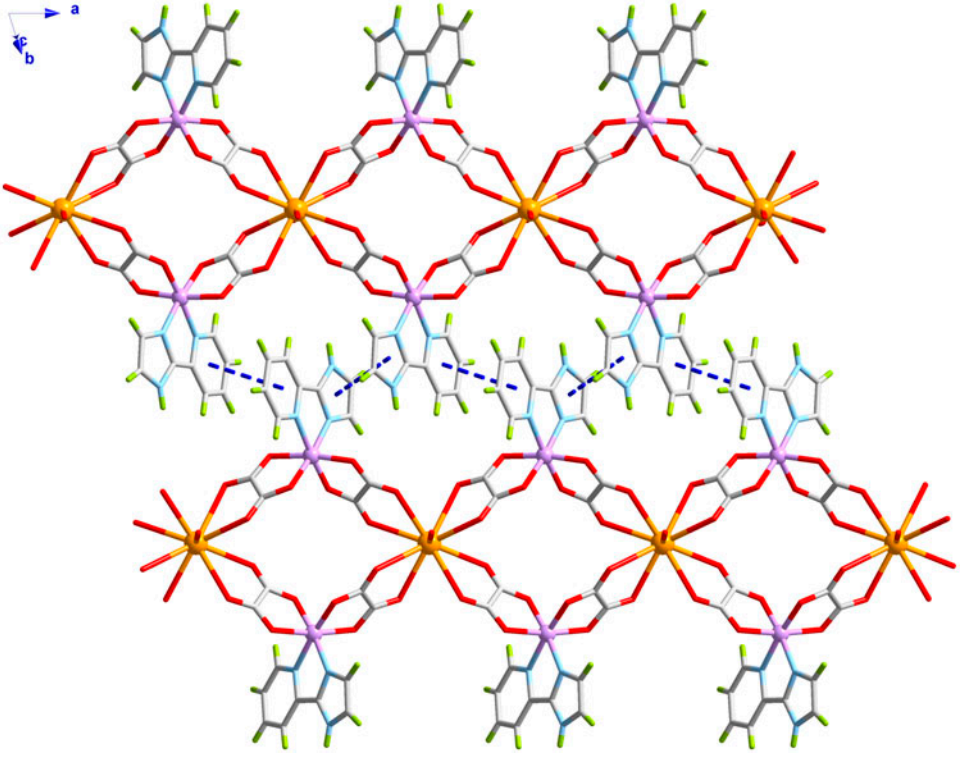

Figure 2. View of the double chain arrangement of **1** along the crystallographic *a* axis showing the π–π type interactions (broken lines) between pyim ligands of adjacent double chains. The crystallization water molecules have been omitted for clarity.

water, the free imidazolyl N–H, and some of the oxalate-oxygens [O···O and N···O distances in the ranges 2.57(2)–3.04(2) and 2.75(3)–2.801(12) Å, respectively] affording a supramolecular 3-D network (figure S2 and table S1).

The two crystallographically independent chromium(III) ions in **1** [Cr(1) and Cr(2)] are six-coordinate by two pyim-nitrogens and four oxygens from two oxalate groups at each metal center in somewhat distorted octahedral surroundings. The reduced values of the angles subtended at the chromium(III) ion by the chelating pyim [79.9(3) (Cr(1)) and 79.6(5)° (Cr(2)] and oxalate ligands [82.9(9) and 82.7(3)° at Cr(1) and 83.5(4), 83.0(4)° at Cr(2)] are the main sources for the distortions from the ideal octahedron. The Cr-N(pyim) [2.021(7) and 2.069(8) Å at Cr(1) and 1.991(12) and 2.050(7) Å at Cr(2)] and Cr-O(oxalate) bond lengths [values in the ranges 1.952(7)–1.977(6) (Cr(1)) and 1.953(8)–1.967(14) Å (Cr(2))] agree with the corresponding values in the mononuclear complexes $XPh_4[Cr(pyim)(C_2O_4)_2]\cdot H_2O$ (X = P and As) [values covering the ranges 2.040(3)–2.101(3) (Cr-N(pyim)) and 1.941(3)–1.959(3) Å (Cr-O(oxalate)] [11].

Each crystallographically independent barium(II) is ten-coordinate by eight oxygens from four bis-bidentate oxalates [values of the Ba-O(oxalate) bond distances vary from 2.741(5)–2.874(7) Å] and two water molecules [values of the Ba-O(water) bond lengths of 2.8385(14) and 2.996(18) Å]. The O–Ba–O bite angles of bridging oxalate are acute [58.49(19)–59.3(2)°]. The barium(II) has a bicapped flattened square antiprism geometry (figure 3), the distance between the basal [O(2)O(6b)O(10)O(14a)] and upper [O(4)O(8b)O(12)O(16a)] mean planes being 2.19(2) Å (compared to an average value of 3.9 Å for their edges). The basal and upper planes are nearly parallel, the value of the dihedral angle between their mean planes being only 2.0(2)°.

The two oxalate ligands in **1** are planar and they adopt the bis(bidentate) coordination mode. The average value of the C–C bond length is 1.54(2) Å, in agreement with its single bond character. The C–O bond distances of the bridging oxalate groups on the side of the chromium(III) ion are somewhat longer [average value 1.28(2) Å] than those at the

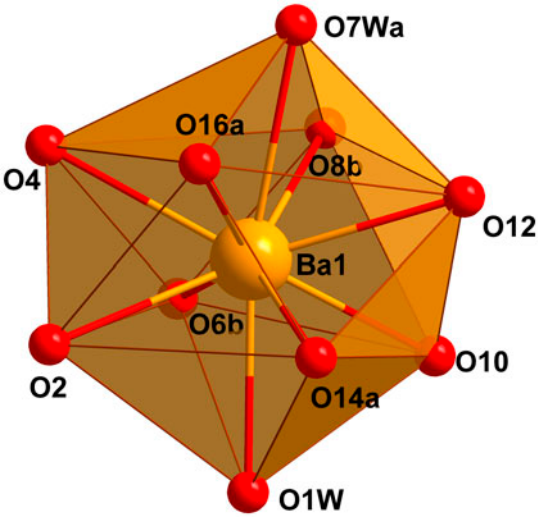

Figure 3. Perspective view of the coordination environment of barium(II) in **1**.

barium(II) center [mean value 1.21(2) Å]. The different nature and charge of the two metal ions account for this asymmetry in the carbonyl-oxalate bonds. The two bidentate pyim molecules are quasi-planar, the values of the dihedral angle between the pyridyl and imidazolyl rings being 7.7(4) [N(1)/N(2)] and 7.6(4)° [N(4)/N(5)]. The values of the dihedral angle between the mean plane of pyim and those of the oxalate groups at the two chromium(III) ions vary in the range 80.6(2)–88.5(2)°, whereas those between adjacent oxalate ligands at each barium center cover the range 55.5(3)–82.4(4)°.

The Cr···Ba separation through the four different oxalate bridges that build the double chains are 6.1539(18) [Cr(1)···Ba(1)], 6.0888(15) [Cr(1)···Ba(1a)], 6.094(3) [Cr(2)···Ba(1)], and 6.018(3) Å [Cr(2)···Ba(1b)]. The shortest interchain Ba···Ba and Cr···Cr distances are 8.8492(14) and 7.003(3) Å, respectively, values which are shorter than the intrachain Ba···Ba [9.6742(12) Å] and Cr···Cr [7.389(3) Å] separations.

3.3. *Magnetic properties of 1*

The magnetic properties of **1** as χ_M against T plot [χ_M is the magnetic susceptibility per one M of Cr(III) ion] in the temperature range 1.9–300 K are shown in figure 4. At room temperature, $\chi_M T$ is ca. 1.86 $cm^3\ M^{-1}$ K, a value which is as expected for a magnetically non-interacting spin quartet ($S_{Cr} = 3/2$). This value remains constant upon cooling until ca. 50 K and further decreases to 1.59 $cm^3\ M^{-1}$ K at 1.9 K. These features are indicative of a very weak antiferromagnetic interaction (θ) between the local spin quartets and/or zero-field splitting effects (D). The shape of the *M versus H* plot for **1** at 2.0 K (see inset of figure 4) agrees with this indication.

In order to evaluate the magnetic interaction in **1**, we have used a simple Curie–Weiss expression [equation (1)],

$$\chi_M = 15N\beta^2 g_{Cr}^2/12k(T-\theta) \quad (1)$$

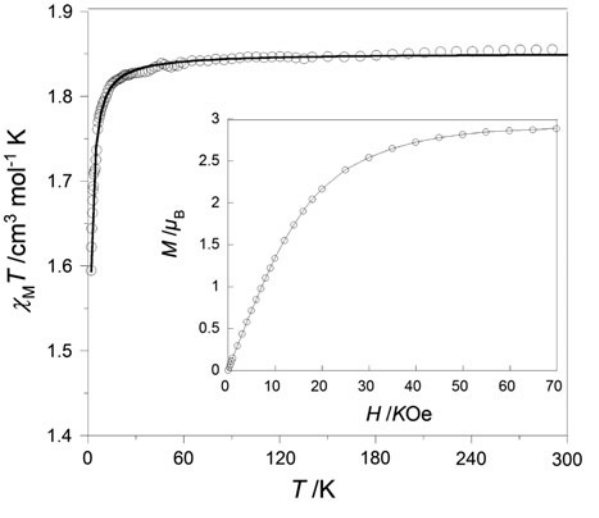

Figure 4. Thermal dependence of $\chi_M T$ for **1**: (o) experimental; (–) best-fit curve through equation (1) (see text). The inset shows the magnetization *vs*. *H* plot for **1** at 2.0 K.

where θ accounts for the magnetic interactions between the Cr(III) centers and g_{Cr} is the average Landé factor of the chromium(III). Least-squares best-fit parameters are $g_{Cr} = 1.987$ and $\theta = -0.32$ K. Given that the D values reported in the literature for six-coordinate mononuclear Cr(III) complexes may reach values up to 1.0 cm^{-1} [25], one could consider that the computed value of θ would be the upper limit for the antiferromagnetic coupling in **1**. However, our attempts to analyze the magnetic data of **1** through the expression derived from the Hamiltonian of equation (2) (case of an axial zero field splitting and $S = 3/2$) [26]

$$H = D[S_z^2 - 1/3(S(S+1))] \tag{2}$$

were unsuccessful. It is clear that the very weak magnetic coupling observed in **1** is in agreement with the large values of the intra- and interchain chromium(III)–chromium(III) separations; a θ value as small −0.05 K was computed for the parent double chain $Ba(H_2O)_2[Cr(dmbipy)(C_2O_4)_2]_2\}_n \cdot 17/2nH_2O$ [10].

3.4. *Protonation/deprotonation equilibria of the pyim (HL) and $[Cr(pyim)(C_2O_4)_2]^-$*

The logarithms of the stepwise protonation constants for the free pyim (HL, scheme 2) and its deprotonation as a ligand in the $[Cr(HL)(C_2O_4)_2]^-$ complex were obtained by electromotive force measurements in water and using 0.15 M $NaNO_3$ as background electrolyte.

Two protonation constants with values of 5.63(1) and 1.41(5) logarithmic units were calculated for the free HL, corresponding to protonation of the imidazole and pyridine rings (see scheme 3).

One acidity constant with pK_a of 7.32(1) was calculated for the chromium(III) complex, which can be attributed to deprotonation of the imidazole ring [equation (3)]:

$$[Cr(HL)(C_2O_4)_2]^- \underset{H^+}{\overset{pK=7.32}{\rightleftharpoons}} [Cr(L)(C_2O_4)_2]^{2-} \tag{3}$$

Based on these data, the corresponding species distribution curves were drawn (figure 5).

To gather more information about the protonation processes of the compounds, the variation of the UV/Vis spectra with pH was monitored. In the case of HL (figure 6), broad spectra were registered, absorbing in the 200–400 nm range. Clear changes upon addition of acid are seen in two different zones of the spectra: one at 210–240 nm leading to an isosbestic point at 224 nm and the other in the 300–400 nm range with an isosbestic point at 332 nm. Insets to these regions, when varying the pH from 7.5 to 3.0, are represented in figure 7. The changes observed correspond to the first protonation step. More acid was added to the solution until reaching a pH of 0.7. The changes observed in the spectrum, related to the second protonation step, can be seen in figure 8.

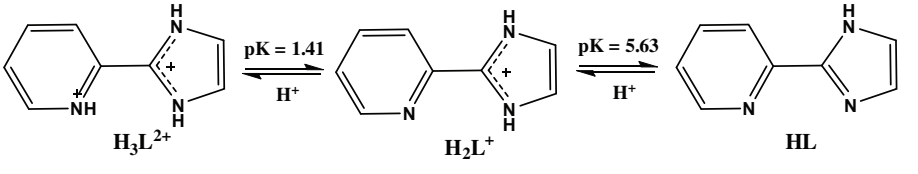

Scheme 3.

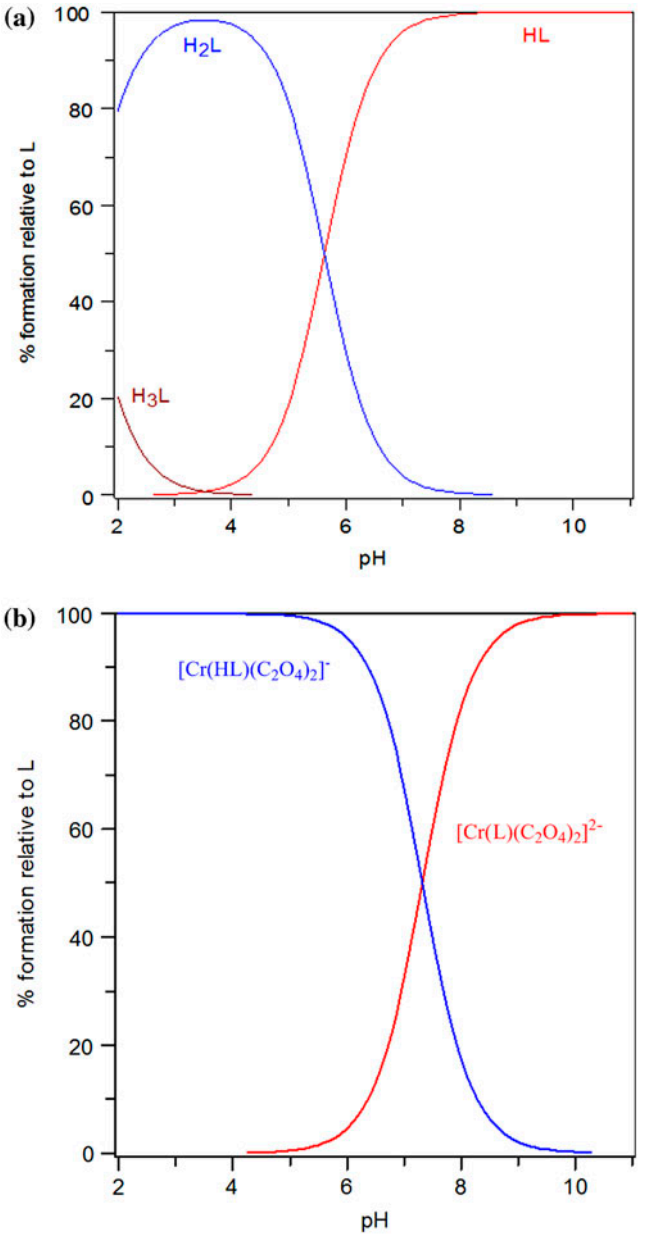

Figure 5. Distribution diagrams for (a) HL and (b) the mixed-ligand complex $[Cr(HL)(C_2O_4)_2]^-$.

We also recorded the UV/Vis of a 0.1 mM $[Cr(HL)(C_2O_4)_2]^-$ solution (figure 9) in the pH range 6.0–11.0. Three isosbestic points are clearly seen. As a result of these spectroscopic measurements, two protonation constants were determined for HL. The logarithm values of the protonation constants, calculated both by EMF and spectroscopic methods, are collected in table 3. The protonation constants reported in the literature for pyridine and imidazole are also included for comparative purposes [27, 28].

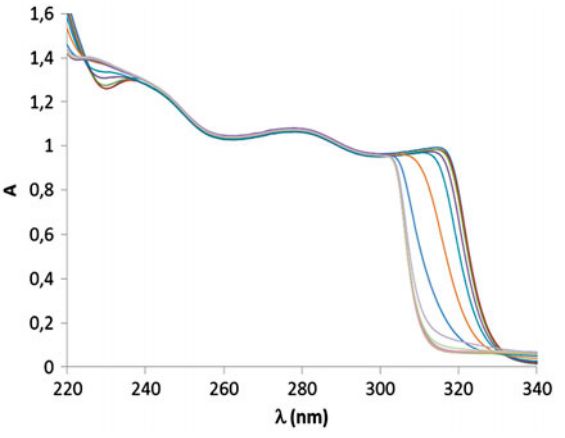

Figure 6. Absorption spectra of 1 mM HL at different pH values (7.0–1.0).

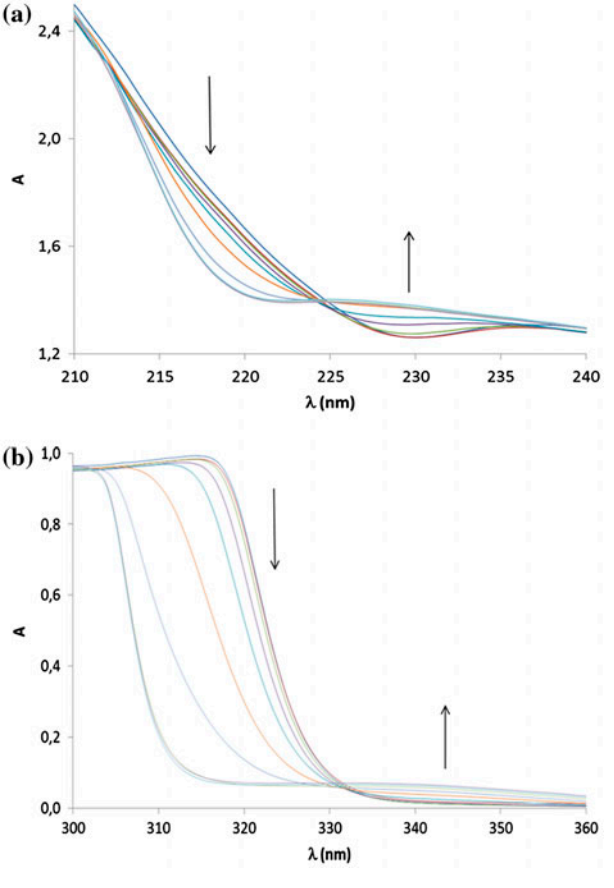

Figure 7. Insets of the absorption spectra of 1 mM HL at pH 7.5–3.0. The arrows show the absorbance changes with increasing amounts of acid.

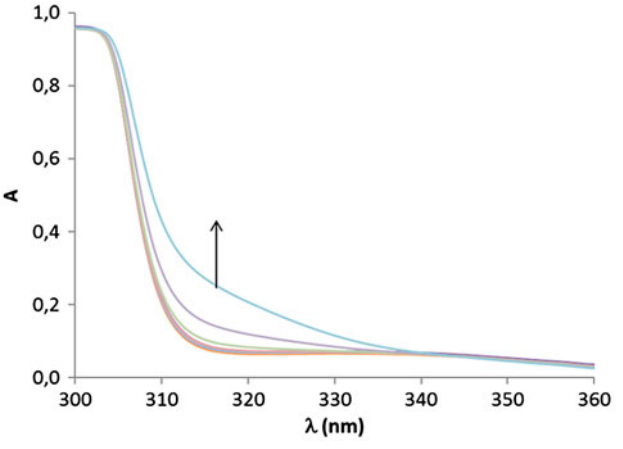

Figure 8. Absorption spectra of 1 mM HL at pH 3.0–0.7. The arrow shows the absorbance change with increasing amounts of acid.

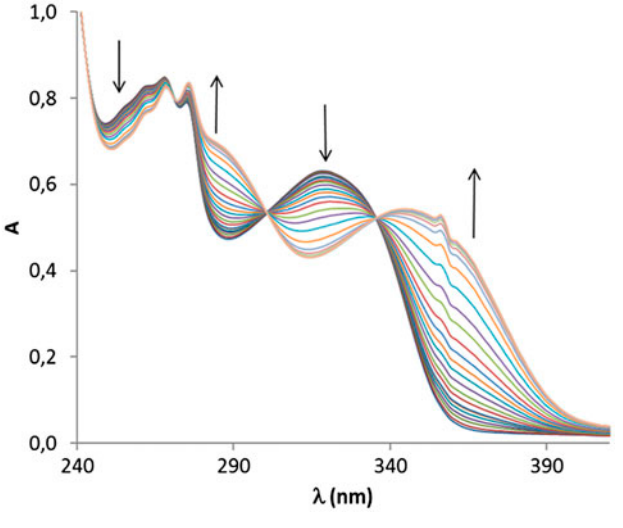

Figure 9. Absorption spectra of 0.1 mM $[Cr(HL)(C_2O_4)_2]^-$ at pH 3.0–0.7. The arrows show the absorbance changes with increasing amounts of acid.

The values of the protonation constants obtained by UV/Vis titrations correspond well with the ones calculated from the pH metric titrations, and the small discrepancies can be easily explained by the fact that no ionic strength was used in the UV/Vis titrations.

Taking into account the data available in the literature [27, 28], the first protonation of HL should take place on the imidazole ring while the second much more acidic one should be affecting the pyridine ring. Comparing with the value from the literature, the pyridinium cation is 3.7 pK units weaker as an acid than the diprotonated ligand. This may be explained in terms of electrostatic repulsion and intramolecular hydrogen bond formation.

In the case of $[Cr(HL)(C_2O_4)_2]^-$, only one acidity constant was determined, both by UV/Vis and EMF titrations with log K_a of 7.6 and 7.3, respectively. The observed process

Table 3. Logarithms of the stepwise protonation constants of the free HL molecule and of the deprotonation of the coordinated HL in $[Cr(HL)(C_2O_4)_2]^-$.

	HL		$[Cr(HL)(C_2O_4)_2]^-$			
Reaction[a]	EMF	UV/Vis	EMF	UV/Vis	Pyridine[c]	Imidazole[d]
$L + H \leftrightarrows HL$	–	–	7.32(1)	7.60(1)	–	14.52
$HL + H \leftrightarrows H_2L$	5.63(1)[b]	5.78(2)	–	–	–	7.05
$H_2L + H \leftrightarrows H_3L$	1.41(5)	1.50(7)	–	–	5.25	–

[a]Charges are omitted for clarity.
[b]Values in parenthesis are standard deviation on the last significant digit.
[c]Value taken from reference [27].
[d]Value taken from reference [28].

should necessarily correspond to the deprotonation of the imidazole ring. It is interesting to note that, in this case, the presence of the coordinated metal increases the acidity of the non-coordinated imidazole nitrogen by seven orders of magnitude, as the deprotonation of the imidazole ring of the coordinated pyim is fully attained at pH ca. 8.4, in contrast with the free imidazole which deprotonates only at pH values higher than 14.

4. Conclusions

A new heterobimetallic oxalate-bridged $Cr^{III}Ba^{II}$ compound has been prepared by direct reaction of the heteroleptic $[Cr(pym)(C_2O_4)_2]^-$ and fully solvated barium(II) in aqueous solution at room temperature. The barium(III) ion is coordinated to eight oxalate oxygens from four oxalate groups and two water molecules; the two crystallographically independent chromium centers within each neutral double chain have opposite chirality. Potentiometric and spectrophotometric studies in aqueous solution show that deprotonation of the free pyim requires strongly basic media, whereas it occurs in slightly basic conditions for the coordinated pyim in $[Cr(pyim)(C_2O_4)_2]^-$ [pK_a = 7.32(1) (emf) and 7.60(1) (UV–Vis)], a very appealing result envisaging the future use of the resulting dianionic species as a ligand through both the oxalate and imidazolate donors.

Supplementary material

Crystallographic data for the structural analysis have been deposited with the Cambridge Crystallographic Data Center; CCDC reference number is 946,980 for **1**. Copies of this information may be obtained free of charge on application to CCDC, 12 Union Road, Cambridge CB2 1EZ, UK (Fax: +44–1223-336–033; E-mail: deposit@ccdc.cam.ac.uk or www: http://ccdc.cam.ac.uk). Supplementary data associated with this article: figures S1, S2 and table S1.

Acknowledgments

The authors are grateful for the financial support of this work provided by the Ministerio Español de Ciencia e Innovación (MICINN) through the projects MAT2010-16981, CTQ2010-15364 and CSD2010-00065 and the Generalitat Valenciana through the project ISIC/2012/002 and

PROMETEO 2011/008. F.R. Fortea-Pérez, J. Vallejo and M. Déniz acknowledge the MICINN for predoctoral fellowships and J. Pasán thanks the Proyecto Estructurante NANOMAC (ACIISI-Gobierno de Canarias) for postdoctoral contract.

References

[1] (a) K.R. Dunbar, R.A. Heintz. *Prog. Inorg. Chem*., **45**, 283 (1997); (b) M. Verdaguer, A. Bleuzen, V. Marvaud, J. Vaissermann, M. Seuleiman, C. Desplanches, A. Scuiller, C. Train, R. Garde, G. Gelly, C. Lomenech, I. Rosenman, P. Veillet, C. Cartier, F. Villain. *Coord. Chem. Rev*., **190-192**, 1023 (1999); (c) M. Ohba, H. Okawa. *Coord. Chem. Rev*., **198**, 313 (2000); (d) J. Cernák, M. Orendác, I. Potocnák, J. Chomic, A. Orendacová, J. Skorsepa, A. Feher. *Coord. Chem. Rev*., **51**, 224 (2002); (e) J. Herrera, V. Marvaud, ; M. Vedaguer, J. Marrot, M. Kalisz, C. Mathonière. *Angew. Chim. Int. Ed*., **43**, 5468 (2004); (f) A. Figuerola, J. Ribas, D. Casanova, M. Maestro, S. Alvarez, C. Díaz. *Inorg. Chem*., **44**, 6949 (2005); (g) S. Tanase, J. Reedijn. *Coord. Chem. Rev*., **250**, 2501 (2006). (h) P. Przychodzen, T. Korzeniak, R. Podgajny, B. Sieklucka. *Coord. Chem. Rev*., **250**, 2234 (2006); (i) J.M. Herrera, P. Franz, R. Podgajny, M. Pilkington, M. Biner, S. Decurtins, H. Stoeckli-Evans, A. Neels, R. Garde, Y. Dromzée, M. Julve, B. Sieclucka, K. Hashimoto, S.I. Okhosho, M. Verdaguer. *C. R. Chimie*, **11**, 1192 (2008); (j) S.A. Stoian, C. Paraschiv, N. Kiritsakas, F. Lloret, E. Münck, E.L. Bominaar. M. Andruh. *Inorg. Chem*., **49**, 3387 (2010).

[2] (a) R. Lescouëzec, L.M. Toma, J. Vaissermann, M. Verdaguer, F.S. Delgado, C. Ruiz-Pérez, F. Lloret, M. Julve. *Coord. Chem. Rev*., **249**, 2691 (2005); (b) M.D. Ward. *Coord. Chem. Rev*., **250**, 3128 (2006); (c) L.M. Toma, L.D. Toma, F.S. Delgado, C. Ruiz-Pérez, J. Sletten, J. Cano, J.M. Clemente-Juan, F. Lloret, M. Julve. *Coord. Chem. Rev*., **250**, 2176 (2006); (d) M. Shatruk, C. Avendano, K.R. Dunbar. *Prog. Inorg. Chem*., **56**, 155 (2009); (e) T.D. Harris, M.V. Bennett, R. Clérac, J.R. Long. *J. Am. Chem. Soc*., **132**, 3980 (2010); (f) F. Karadas, C. Avendano, M.G. Hilfiger, A.V. Prosvirin, K.R. Dunbar. *Dalton Trans*, 4968 (2010); (g) S. Wang, X.H. Ding, J.L. Zuo, X.Z. You, W. Huang. *Coord. Chem. Rev*., **255**, 1713 (2011); (h) X. Feng, J. Liu, T.D. Harris, S. Hill, J.R. Long. *J. Am. Chem. Soc*., **134**, 7521 (2012); (i) S. Wang, X.H. Ding, Y.H. Li, W. Huang. *Coord Chem. Rev*., **256**, 439 (2012). (j) Y.H. Li, W.R. He, X.H. Ding, S. Wang, L.F. Cui, W. Huang. *Coord Chem. Rev*., **256**, 2795 (2012).

[3] (a) S. Decurtins, R. Pellaux, G. Antorrena, F. Palacio. *Coord. Chem. Rev*., **190-192**, 841 (1999); (b) E. Coronado, J.R. Galán-Mascarós, C.J. Gómez-García, V. Laukhin. *Nature*, **408**, 447 (2000); (c) M. Pilkington, S. Decurtins. In Comprehensive Coordination Chemistry II, J.A. McCleverty, T.J. Meyers (Eds.), Vol. 7, p. 177, Elsevier, Amsterdam (2004); (d) M. Gruselle, C. Train, K. Boubekeur, P. Gredin, N. Ovanesyan. *Coord. Chem. Rev*., **250**, 2491 (2006); (e) J. Martínez-Lillo, D. Armentano, G. De Munno, W. Wernsdorfer, M. Julve, F. Lloret, J. Faus. *J. Am. Chem. Soc*., **128**, 14218 (2006); (f) C. Train, R. Gheorghe, V. Krstic, L.M. Chamoreau, N.S. Ovanesyan, L.J.A. Rikken, M. Gruselle, M. Verdaguer. *Nat. Mater*., **9**, 729 (2008); (g) C. Train, T. Nuida, R. Gheorghe, M. Gruselle, S.I. Ohkoshi. *J. Am. Chem. Soc*., **131**, 16838 (2009); (h) H. Okawa, A. Shigematsu, M. Sadakiyo, T. Miyagawa, K. Yoneda, M. Ohba, H. Kitagawa. *J. Am. Chem. Soc*., **131**, 13516 (2009); (i) E. Pardo, C. Train, G. Gontard, K. Boubekeur, O. Fabelo, H. Liu, B. Dkhil, F. Lloret, K. Nakagawa, H. Tokoro, S.I. Ohkoshi, M. Verdager. *J. Am. Chem. Soc*., **133**, 15328 (2011); (j) M. Clemente-León, E. Coronado, C. Martí-Gastaldo, F.M. Romero. *Chem. Soc. Rev*., **40**, 473 (2011); (k) C. Train, M. Gruselle, M. Verdaguer. *Chem. Soc. Rev*., **40**, 3297 (2011); (l) E. Pardo, C. Train, K. Boubekeur, G. Gontard, J. Cano, F. Lloret, K. Nakatani, M. Verdaguer. *Inorg. Chem*., **51**, 11582 (2012); (m) E. Pardo, C. Train, H. Liu, L.M. Chamoreau, B. Dkhil, K. Boubekeur, F. Lloret, K. Nakatani, H. Tokoro, S.I. Okoshi, M. Verdaguer. *Angew. Chem. Int. Ed*., **51**, 8356 (2012).

[4] (a) E. Pardo, R. Ruiz-García, J. Cano, X. Ottenwaelder, R. Lescouëzec, Y. Journaux, F. Lloret, M. Julve. *Dalton Trans.*, 2780 (2008); (b) M.C. Dul, E. Pardo, R. Lescouëzec, Y. Journaux, J. Ferrando-Soria, R. Ruiz-García, J. Cano, M. Julve, F. Lloret, D. Cangussu, C.L.M. Pereira, H.O. Stumpf, J. Pasán, C. Ruiz-Pérez. *Coord. Chem. Rev.*, **254**, 2281 (2010); (c) J. Ferrando-Soria, D. Cangussu, M. Eslava, Y. Journaux, R. Lescouëzec, M. Julve, F. Lloret, J. Pasán, C. Ruiz-Pérez, E. Lhotel, C. Paulsen, E. Pardo. *Chem. Eur. J.*, **17**, 12482 (2011); (d) J. Ferrando-Soria, R. Ruiz-García, J. Cano, S.E. Stririba, J. Vallejo, I. Castro, M. Julve, F. Lloret, P. Amorós, J. Pasán, C. Ruiz-Pérez, Y. Journaux, E. Pardo. *Chem. Eur. J.*, **18**, 1608 (2012); (e) J. Ferrando-Soria, P. Serra-Crespo, M. de Lange, J. Gascon, F. Kapteijn, M. Julve, J. Cano, F. Lloret, J. Pasán, C. Ruiz-Pérez, Y. Journaux, E. Pardo. *J. Am. Chem. Soc.*, **134**, 15301 (2013); (f) J. Ferrando-Soria, H. Khajavi, P. Serra-Crespo, J. Gascon, F. Kapteijn, M. Julve, F. Lloret, J. Pasán, C. Ruiz-Pérez, Y. Journaux, E. Pardo. *Adv. Mater.*, **24**, 5625 (2012); (g) F.R. Fortea-Pérez, J. Vallejo, M. Julve, F. Lloret, G. De Munno, D. Armentano, E. Pardo. *Inorg. Chem.*, **52**, 4777 (2013).

[5] (a) G. Marinescu, M. Andruh, F. Lloret, M. Julve. *Coord. Chem. Rev*., **255**, 161 (2010); (b) J. Vallejo, I. Castro, L. Cañadillas-Delgado, C. Ruiz-Pérez, J. Ferrando-Soria, R. Ruiz-García, J. Cano, F. Lloret, M. Julve. *Dalton Trans*, 2350 (2010); (c) J. Vallejo, I. Castro, J. Ferrando-Soria, M. Déniz-Hernández, C. Ruiz-Pérez, F. Lloret, M. Julve, R. Ruiz-Pérez, J. Cano. *Inorg. Chem*., **50**, 2073 (2011); (d) J. Vallejo, I. Castro, M. Déniz, C. Ruiz-Pérez, F. Lloret, M. Julve, R. Ruiz-García, J. Cano. *Inorg. Chem*., **51**, 3289 (2012).

[6] (a) G. De Munno, D. Armentano, M. Julve, F. Lloret, R. Lescouëzec, J. Faus. *Inorg. Chem*., **38**, 2234 (1999); (b) F. Bérézovsky, A.A. Hajem, S. Triki, J.S. Pala, P. Molinié. *Inorg. Chim. Acta*, **284**, 8 (1999).
[7] (a) M.C. Muñoz, M. Julve, F. Lloret, J. Faus, M. Andruh. *J. Chem. Soc., Dalton Trans*., 3125 (1998); (b) G. Marinescu, M. Andruh, R. Lescouëzec, M.C. Muñoz, J. Cano, F. Lloret, M. Julve. *New J. Chem*., **24**, 527 (2000); (c) F.D. Rochon, G. Massarweh. *Can. J. Chem*., **77**, 2059 (1999).
[8] (a) F.D. Rochon, R. Melanson, M. Andruh. *Inorg. Chem*., **35**, 6086 (1996); (b) G. Marinescu, M. Andruh, M. Julve, F. Lloret, R. Llusar, S. Uriel, J. Vaissermann. *Cryst. Growth Des*., **5**, 261 (2005).
[9] R. Lescouëzec, G. Marinescu, M.C. Muñoz, D. Luneau, M. Andruh, F. Lloret, J. Faus, M. Julve, J.A. Mata, R. Llusar, J. Cano. *New J. Chem.*, **25**, 1224 (2001).
[10] M. Viciano-Chumillas, N. Marino, I. Sorribes, C. Vicent, F. Lloret, M. Julve. *Cryst. Eng. Comm.*, **12**, 122 (2010).
[11] O. Schott, J. Ferrando-Soria, A. Bentama, S.E. Stiriba, J. Pasán, C. Ruiz-Pérez, M. Andruh, F. Lloret, M. Julve. *Inorg. Chim. Acta*, **376**, 358 (2011).
[12] A. Earnshaw. *Introduction to Magnetochemistry*., Academic Press, London (1968).
[13] E. García-España, M.J. Ballester, F. Lloret, J.M. Moratal, J. Faus, A. Bianchi. *J. Chem. Soc., Dalton Trans*., 101 (1988).
[14] M. Fontanelli, M. Micheloni, Program for the automatic control of the microburette and the acquisition of the electromotive force readings, Proceedings of the I Spanish-Itaian Congress on Thermodynamics of Metal Complexes, Diputación de Castellón, Castellón, Spain (1990).
[15] (a) G. Gran. *Analyst* (London), **77**, 661 (1952); (b) F.I. Rossotti, H. Rossotti. *J. Chem. Educ*., **42**, 375 (1965).
[16] P. Gans, A. Sabatini, A. Vacca. *Talanta*, **43**, 1739 (1996).
[17] Agilent. *CrysAlisPRO Agilent Technologies*., Yarnton, England (2012).
[18] G.M. Sheldrick. *Acta Cryst.*, **A64**, 112 (2008).
[19] L.J. Farrugia. *J. Appl. Cryst.*, **32**, 837 (1999) (WINGX).
[20] M. Nardelli. *J. Appl. Cryst.*, **28**, 659 (1995).
[21] DIAMOND 2.1d, Crystal Impact GbR, K. Brandenburg and H. Putz GbR, Postfach 1251, D-53002 Bonn, Germany (2000).
[22] K. Nakamoto. *Infrared and Raman Spectra of Inorganic and Coordination Compounds*, 4th Edn, p. 228, Wiley, New York (1986).
[23] P. Sharma, H.S. Virk. *The Open Surface Science Journal*, **1**, 34 (2009).
[24] J.R. Ferraro, R. Driver, W.R. Walker, W. Wozniak. *Inorg. Chem.*, **6**, 1586 (1967).
[25] R. Boca. *Coord. Chem. Rev.*, **248**, 757 (2004).
[26] C.J. O'Connor. *Prog. Inorg. Chem.*, **29**, 203 (1982).
[27] R.G. Pearson, F.V. Williams. *J. Am. Chem. Soc.*, **75**, 3073 (1953).
[28] H. Walba, R.W. Isensee. *J. Org. Chem.*, **26**, 2789 (1961).